Electrochemical quantification of Ag_2S Quantum Dots: evaluation of different surface coating ligands for bacteria determination

*Olaya Amor-Gutiérrez[1], Alba Iglesias-Mayor[1], Pablo Llano-Suárez[2], José M. Costa-Fernández[2], Ana Soldado[3], Ana Podadera[4], Francisco Parra[4], Agustín Costa-García[1], Alfredo de la Escosura-Muñiz[1]**

[1] NanoBioAnalysis Group-Department of Physical and Analytical Chemistry, University of Oviedo, Julián Clavería 8, 33006, Oviedo, Spain

[2] Department of Physical and Analytical Chemistry, University of Oviedo, Julián Clavería 8, 33006, Oviedo, Spain

[3] Department of Animal Nutrition, Grassland and Forages, Regional Institute for Research and Agro-Food Development (SERIDA), Villaviciosa, Asturias, Spain

[4] Instituto Universitario de Biotecnología de Asturias, Departamento de Bioquímica y Biología Molecular, Edificio Santiago Gascón, Universidad de Oviedo, Campus El Cristo, 33006 Oviedo, Spain

*Corresponding author. E-mail address: alfredo.escosura@uniovi.es

ORCID ID: 0000-0002-9600-0253

Phone: +34985103521

ABSTRACT

In this work, novel silver sulphide Quantum Dots (Ag_2S QD) are electrochemically quantified for the first time. The method is based on the electrochemical reduction of Ag^+ to Ag^0 at -0.3 V on screen-printed carbon electrodes (SPCEs), followed by anodic stripping voltammetric oxidation that gives a peak of currents at +0.06 V which represents the analytical signal. The optimized methodology allows the quantification of water-stabilized Ag_2S QD in the range of approximately 2×10^9-2×10^{12} QD·mL^{-1} with a good reproducibility (RSD: 5%). Moreover, as proof-of-concept of relevant biosensing application, Ag_2S QD are evaluated as tags for *Escherichia coli* (*E. coli*) bacteria determination. Bacteria tagged with QD are separated by centrifugation from the sample solution and placed on the SPCE surface for quantitative analysis. The effect of two different Ag_2S QD surface coating/stabilizing agents on both the voltammetric response and the bacteria sensing is also evaluated. 3-mercaptopropionic acid (3-MPA) is studied as model of short length coating ligand with no affinity for the bacteria, while boronic acid (BA) is evaluated as longer length ligand with chemical affinity for the polysaccharides present in the peptidoglycan layer on the bacteria cells surface. The biosensing system allows to detect bacteria in the range 10^{-1}-10^3 bacteria·mL^{-1} with a limit of detection as low as 1 bacteria·mL^{-1} This methodology is a promising proof-of-concept alternative to traditional laboratory-based tests, with good sensitivity and short time and low cost of analysis.

KEYWORDS

Silver sulphide, quantum dots, electrochemical determination, anodic stripping voltammetry, bacteria quantification, *E. coli*

1. INTRODUCTION

Among the wide variety of nanomaterials, so much attention is currently given to Quantum Dots (QD), semiconductor nanocrystals with different photoluminescent and semiconductive properties. QD were discovered around 1980s by Alexey Ekimov [1, 2] when studying different semiconductor nanocrystals. QD are good candidates to be used as labels in assays, [3] thanks to their high photoluminescence emission quantum yields, narrow spectral bands or size-tunable emission profiles, between other properties. [4] Different coating surfaces can be used to control their solubility and functionalization [5] with the aim of using them in different types of assays. [6] QD detection/characterization is generally carried out with techniques such as photoluminescence techniques, inductively coupled plasma mass spectrometry (ICP-MS), X-ray diffraction, X-ray photoelectron spectroscopy or electron microscopy. [7, 8] However, these powerful techniques have considerable limitations related either sometimes to the reduced sensitivity or to the time and cost of analysis.

Electrochemical methods are a worthwhile alternative for the QD analysis taking advantage of faster and cheaper procedures, providing valuable information about the nanocrystals. [9, 10] QD were electrochemically studied for the first time in 2005 by Bard's group, [11] being then employed as electrochemical labels for the first time by Joseph Wang and co-workers [12] and extensively used from then. [13]

Typical QD containing heavy metals, such as Cd, Te or Pb have well-known fluorescent properties with a characteristic emission in the ultraviolet (UV) and visible (Vis) regions. Size-tunable and narrow emission, efficient light absorption throughout a wide spectrum, high quantum yields with exceptional resistance to

photobleaching are some of the outstanding features of conventional QD, making these materials very attractive to be used in photoluminescent analytical applications. Research in the synthesis and characterization of near infrared (NIR)-emitting QD provides exciting opportunities in (bio)nanotechnology. [14] NIR-emitting QD have many advantages for potential biosensing/biodetermination applications, related to the high quantification sensitivity, low fluorescent background signals, and low matrix effects in biological media, since many biological species emit on the ultraviolet-visible range. [14, 15]

In this context, we reported the synthesis and characterization of NIR fluorescent silver sulplhide (Ag_2S) QD and their application as nanoprobes for optical assays. [16] However, to the best of our knowledge, the electrochemical properties of such Ag_2S QD haven't been neither studied nor exploited for biodetermination purposes. In this scenario, we report the electrochemical determination of Ag_2S QD based on anodic stripping voltammetry and their application as tags for bacteria quantification, taking advantage of the affinity of silver for cell surface macromolecules. Such bacteria determination is an emerging hot topic, due to the increasing resistance of bacteria to antimicrobial agents and the limitations of traditional methods of analysis based on cell culturing. [17, 18]. The effect of different QD surface coatings on both the electroactive properties of the Ag_2S QD and the assay performance is also studied and discussed.

2. EXPERIMENTAL

2.1. Chemicals and equipment

The precursors used for the synthesis of the Ag_2S QD were: 3-mercaptopropionic acid (3-MPA, ≥ 99%), silver nitrate (> 99%), sodium sulphide nonahydrate (≥ 98%), sodium hydroxide, 3-aminophenylboronic acid, N-(3-dimethylaminopropyl)-N′-ethylcarbodiimide hydrochloride (EDC), N-hydroxysuccinimide (NHS, 98%), all of them purchased from Sigma-Aldrich (www.sigmaaldrich.com), part of Merck KGaA (Germany). Acetic acid glacial was purchased from Fisher (www.thermofisher.com), part of Thermo Fischer Scientific (Belgium).

For the electrochemical measurements, fuming hydrochloric acid (37%) was also obtained from Merck KGaA (www.merckgroup.com) (Germany).

The bacteria used were *Escherichia coli*: XL1-blue (*rec*A1 *end*A1 *gyr*A96 *thi*-1 *hsd*R17 *sup*E44 *rel*A1 *lac* [*F' proAB lacI*^{q} *ZΔM15* Tn*10* (Tet^r)] purchased from Agilent (https://www.agilent.com) (United States of America) and *Salmonella typhimurium* strain LT2 (American Type Culture Collection, ATCC, number 700720). Bacteria cultures were made using Luria-Bertani (LB) broth medium and phosphate buffered saline (PBS) from Sigma-Aldrich (www.sigmaaldrich.com) and a B. Braun Biotech Certomac IS orbital incubator from B. Braun Biotech International GmbH (Germany). Humic acid was purchased from Sigma-Aldrich (www.sigmaaldrich.com). Human serum from healthy patients was kindly provided by Cabueñes Hospital (Gijón, Asturias, Spain).

A MSC-100 cooling thermoshaker incubator purchased from Labolan (www.labolan.es) (Spain) was used for the incubation of the Ag_2S QD with *bacteria cell cultures*. The suspensions were centrifuged using a ROTANTA 460 R thermostatic centrifuge from Hettich (www.hettichlab.com) (Germany).

All chemical reagents were of analytical grade and used as received without further purification. All the solutions were prepared in ultrapure water (18.2 MΩ) obtained with a Millipore Direct-Q® 3 UV purification system from Millipore Ibérica S.A (Spain).

Preconcentration and purification of the Ag_2S QD with the different coatings was carried out using 3-kDa Amicon-Ultra centrifugal filters from Merck KGaA, (www.merckmillipore.com) (Germany).

Photoluminescence properties of the synthesized QD were studied using a Varian Cary Eclipse Fluorescence Spectrometer from Varian Ibérica (www.agilent.com) (Spain) equipped with a xenon discharge lamp (peak power equivalent to 75 kW), a Czerny-Turner monochromator and a photomultiplier tube detector (Model R-298). Fluorescence spectra were recorded using a fixed excitation wavelength of 530 nm with both excitation and emission slits widths of 10 nm. All measurements were made at constant temperature (20 °C) and atmospheric pressure, using quartz cuvettes from Hellma (www.hellma-analytics.com) (Germany).

In order to study the purity of the QD, Asymmetric Flow-Field Flow Fractionation (AF4) was on-line coupled to Inductively Coupled Plasma Mass Spectrometry (ICP-MS). Silver elemental analysis was performed using ICP-MS. For this purpose, a Triple Quad 8800 ICP-QQQ from Agilent (www.agilent.com) (Japan)

with a concentric nebulizer with double-pass glass spray chamber Scott type was used. Operation conditions for the ICP-MS analysis were optimized using a tuning solution. Elemental Ag was measured in on-mass MS/MS mode (107 Ag+). The integration time for each of the targeted isotopes was 100 ms.

High Resolution Transmission Electron Microscopy (HR-TEM) images were acquired using a JEM 2100 instrument from JEOL (www.jeol.co.jp) (Japan), which operates at an accelerating voltage of 200 kV. Samples were prepared by placing several drops of diluted QD suspension in ultrapure water onto a carbon coated copper TEM grid and then allowed to air-dry before loading in the microscope.

In order to have homogeneous dispersions of nanoparticles, an Elmasonic P 30 H ultrasonic bath from Elma Schmidbauer GmbH (www.elma-ultrasonic.com) (Germany) was used. Electrochemical measurements were carried out using an µAutolab type II potentiostat/galvanostat from Eco Chemie (www.ecochemie.nl) (The Netherlands) interfaced to a computer system and controlled by the NOVA version 2.1 software from Metrohm Autolab (www.metrohm-autolab.com) (The Netherlands). Screen-printed carbon electrodes (SPCEs, ref. DRP-110) and their connector for the potentiostat (ref. DSC) were purchased from Metrohm DropSens (www.dropsens.com) (Spain). The conventional three-electrode configuration of SPCEs includes both carbon working and counter electrodes and a silver pseudoreference electrode. All measurements were carried out at room temperature.

2.2. Methods

2.2.1. Synthesis and characterization of Ag_2S QD with different surface coatings

Ag_2S QD were synthesized following a procedure previously reported by our group. [16] First, in the case of the 3-mercaptopropionic acid-silver sulphide quantum dots (3-MPA-Ag_2S QD), 3-mercaptopropionic acid (3-MPA, 0.14 g) was dissolved in deionized water (50 mL), being the pH of this solution adjusted to 7.5 with 1 M sodium hydroxide and 1 M acetic acid solutions. Then, silver nitrate ($AgNO_3$, 42.5 mg) was added, and the pH was adjusted again to 7.5. The solution was spilled in a three-necked flask, deoxygenated with argon and covered with aluminium foil, to avoid light exposure. The mixture was heated to 50 °C while a deoxygenated sodium sulphide solution (13.9 mg of sodium sulphide in 20 mL of deionized water) was slowly added under continuous and vigorous stirring. After that, it was left to react for 7 h at 50 °C.

In order to obtain boronic acid-silver sulphide quantum dots (BA-Ag_2S QD), 3-MPA-Ag_2S QD were preconcentrated using a 3-kDa Amicon-Ultra centrifugal filters. Then, they were bioconjugated with 3-aminophenylboronic acid following the well-known EDC carbodiimide crosslinking reaction in the presence of sulfo-NHS to increase the bioconjugation efficiency through the generation of a stable sulfo-NHS ester intermediate reaction. [19] A volume of 10 mL of 100 nM 3-MPA-Ag_2S QD was made to react together with 0.025 mM EDC (0.3 mL) and 0.015 mM NHS (0.2 mL) during 2 h. After that, 3 mL of 0.025 mM 3-aminophenylboronic acid was added to the mixture and left to react 4 h. This reaction was made at room temperature and under continuous mechanical stirring.

The synthesized Ag_2S QD (3-MPA-Ag_2S QD and BA-Ag_2S QD) were purified using a 3-kDa Amicon-Ultra centrifugal filters and washing with ultrapure water several times. All the solutions were stored protected from light at 4 °C.

HR-TEM images were acquired in order to evaluate the Ag_2S QD size and shape as well as the absence of aggregates. The characteristic fluorescence emission of the Ag_2S QD at approximately 800 nm (λ_{ex} = 530 nm) was also recorded to corroborate the correct QD formation.

2.2.2. Electrochemical determination of Ag_2S QD

In order to obtain homogeneous dispersions of Ag_2S QD, the stock solutions were first sonicated for 5 min in an ultrasonic bath (frequency: 30-100 Hz, temperature: 25 °C). After that, 5 µL of QD solution at different concentrations were deposited on the working electrode and allowed to dry at room temperature, for approximately 30 min. Electrochemical quantification was performed by placing 40 µL of 0.1 M HCl on the Ag_2S QD-modified SPCE and applying a constant reductive potential of -0.3 V for 60 s. Then, the hydrogen that may have been formed on the electrode surface was desorbed by applying a constant potential of -0.1 V for 60 s. After that, a scan to oxidative potentials from -0.1 V to +0.3 V was applied using cyclic voltammetry (CV) at a scan rate of 50 $mV \cdot s^{-1}$. The value of the peak current recorded at approximately +0.06 V is considered as the analytical signal.

It's worthy to note that the constant background of 0.8 µA coming from the silver present in the printed reference electrode (see optimization studies at the ESM) was subtracted from all the analytical signals (both of Ag_2S QD and bacteria analysis) under the optimized experimental conditions.

All measurements were done by triplicate. Removal of oxygen from the solution was not necessary. A new SPCE was used for each measurement.

2.2.3. Escherichia coli culture

E. coli XL1-blue cells were aerobically cultured at 37 ºC in sterile Erlenmeyer flasks containing 100 mL LB Broth medium, using an orbital incubator at 250 rpm. After overnight incubation, the cultures reached an absorbance at 600 nm (A_{600nm}) of 2.54 and bacteria cells were harvested by centrifugation. After the centrifugation, the sediments were washed using PBS (pH 7.5) and the bacteria pellet was re-suspended in 10 mL of PBS. Assuming that one unit of A_{600nm} of an *E. coli* suspension contains approximately 1.00×10^{8} bacteria·mL^{-1} that amount is considered as *E. coli* concentration of the stock bacteria solution.

2.2.4. Incubation of E. coli bacteria with Ag_2S QD and electrochemical quantification

The incubation of the Ag_2S QD with *E. coli* bacteria was carried out by mixing 500 µL of 1.80×10^{12} QD·mL^{-1} (for both 3-MPA-Ag_2S QD and BA-Ag_2S QD) with 500 µL of suspensions with different amounts of *E. coli* (concentrations between 10^{-1} and 10^{7} bacteria·mL^{-1}) and incubating at 37 °C for 30 min under gentle stirring. After that, the suspensions were centrifuged at 1700g (20 °C, 10 min) for removing the excess of Ag_2S QD. The resulting pellet was re-suspended in 50 µL of milli-Q water, deposited on the SPCE working electrode surface and kept there for 2 minutes, as previously optimized. [20] Finally, the electrochemical determination of the Ag_2S QD linked to the bacteria was performed following the experimental procedure described in section 2.2.2, studying the variation in the peak current at +0.06 V for different concentrations of *E. coli* cells.

2.2.5. Selectivity and specificity studies

To test the selectivity of the detection strategy, *Salmonella* bacteria cells were incubated with the Ag_2S QD, as described in section 2.2.4. *Salmonella* cells were cultured as described for *E. coli* bacteria, in this case a value of 2.96 of A_{600nm} indicates a bacterial density of around 4.30×10^{11} bacteria·mL^{-1}.

To test the specificity in presence of potential interference compounds, the assay was performed over a suspension of 10^2 *E. coli* bacteria·mL^{-1} in presence of human serum and humic acid (4 mg·L^{-1}).

3. RESULTS AND DISCUSSION

3.1. Characterization of 3-MPA-Ag_2S QD and BA-Ag_2S QD

Two different Ag_2S QD surface coating/stabilizing agents were evaluated for the further bacteria quantification. 3-mercaptopropionic acid (3-MPA) was studied as model of short length coating ligand with no affinity for bacteria while boronic acid (BA) was evaluated as longer length ligand with chemical affinity for the polysaccharides present in the peptidoglycan layer on the surface of bacteria cells.

Ag_2S QD synthesized with the two different surface coatings were first evaluated by HR-TEM (**Fig. 1**). The images show that in both cases the Ag_2S QD has a spherical shape. However, different nanoparticle sizes were found depending on the surface coating, being the average diameters of 6 ± 1 nm for the 3-MPA-Ag_2S QD (**Fig. 1a**) and 9 ± 2 nm for the BA-Ag_2S QD (**Fig. 1b**) (histograms are given

in **Fig. A1** at the ESM). Such difference noticed is in correlation with the longer length of the BA ligand compared with the 3-MPA one, as schematized in **Fig. 1.**

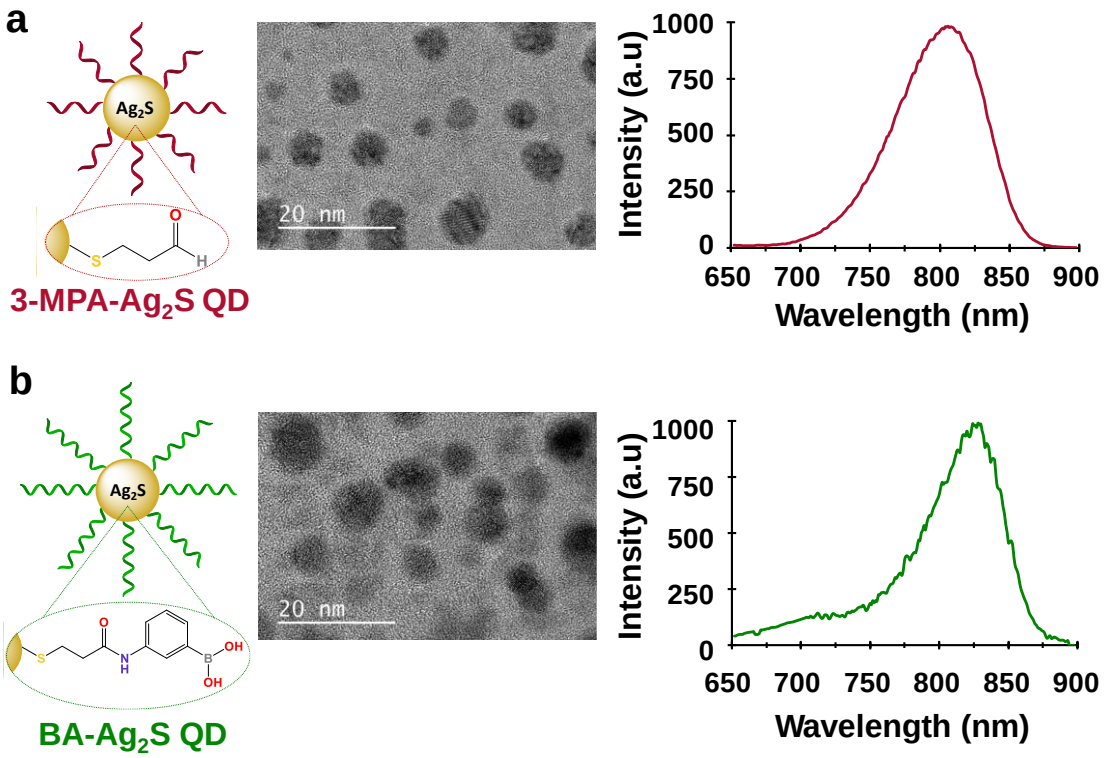

Fig. 1 From left to right: Schematic representation of the Ag_2S QD synthesized with different surface coatings, HR-TEM images and fluorescence emission spectra (λ_{ex} = 530 nm) for **(a)** 3-mercaptopropionic acid Ag_2S QD (3-MPA-Ag_2S QD) and **(b)** boronic acid Ag_2S QD (BA-Ag_2S QD)

Fluorescence properties were also evaluated, exciting at 530 nm. Fluorescence emissions centred at wavelengths of 806 nm for 3-MPA-Ag_2S QD (**Fig. 1a**) and of 827 nm for BA-Ag_2S QD (**Fig. 1b**) were found, as expected**.** Such emission property, within the near infrared region (700-2500 nm) is characteristic of these QD, as previously reported by our group. [16]

A crucial parameter for the analytical application of the QD is the nanoparticle concentration. Ag_2S QD concentration was calculated considering the size (determined by HR-TEM), the stoichiometry (obtained from X-Ray Diffraction (XRD) analysis) and the nanoparticle number concentration (determined by ICP-

MS). Accuracy of such approach depends on the purity of the sample. It is necessary to confirm that all the Ag quantified came from the Ag_2S QD and not from unreacted silver precursor or any other concomitant nanoparticulated species generated during the synthesis (e.g. AgNPs). Analysis by AF4-ICP-MS of the purified product from the synthesis resulted in a fractogram in which only a single narrow peak was detected, where Ag and S ions were simultaneously detected, thus confirming the presence of Ag_2S NP and the absence of free ionic Ag^+ or other concomitant nanoparticulated Ag species. Considering all those factors, the concentration of the synthesized QD is estimated to be 2.20×10^{14} $QD\cdot mL^{-1}$ for 3-MPA-Ag_2S QD and 1.80×10^{14} $QD\cdot mL^{-1}$ for BA-Ag_2S QD.

3.2. Electrochemical determination of Ag_2S QD

3.2.1. Voltammetric monitoring of Ag_2S QD

Electrochemical quantification of Ag_2S QD was performed by anodic stripping voltammetry. As illustrated in **Fig. 2**, such procedure consists in the electrochemical reduction of the Ag^+ present in the surface of the QD to Ag^0. This reduction leads to a pre-concentration of silver on the electrode, being actually such characteristic the main contributor to the high sensitivity of the stripping analysis. After that, Ag^0 is re-oxidized back to Ag^+ by scanning to positive potentials, recording at approximately +0.06 V the peak of current characteristic of the oxidation of Ag^0 to Ag^+. The value of such peak current is considered as the analytical signal which allows the QD quantification. Hydrochloric acid plays a key role here, being the source of Cl^- ions that form the AgCl complex with the

re-oxidized Ag^+. The formation of this complex facilitates the silver re-oxidation process and consequently the electrochemical quantification.

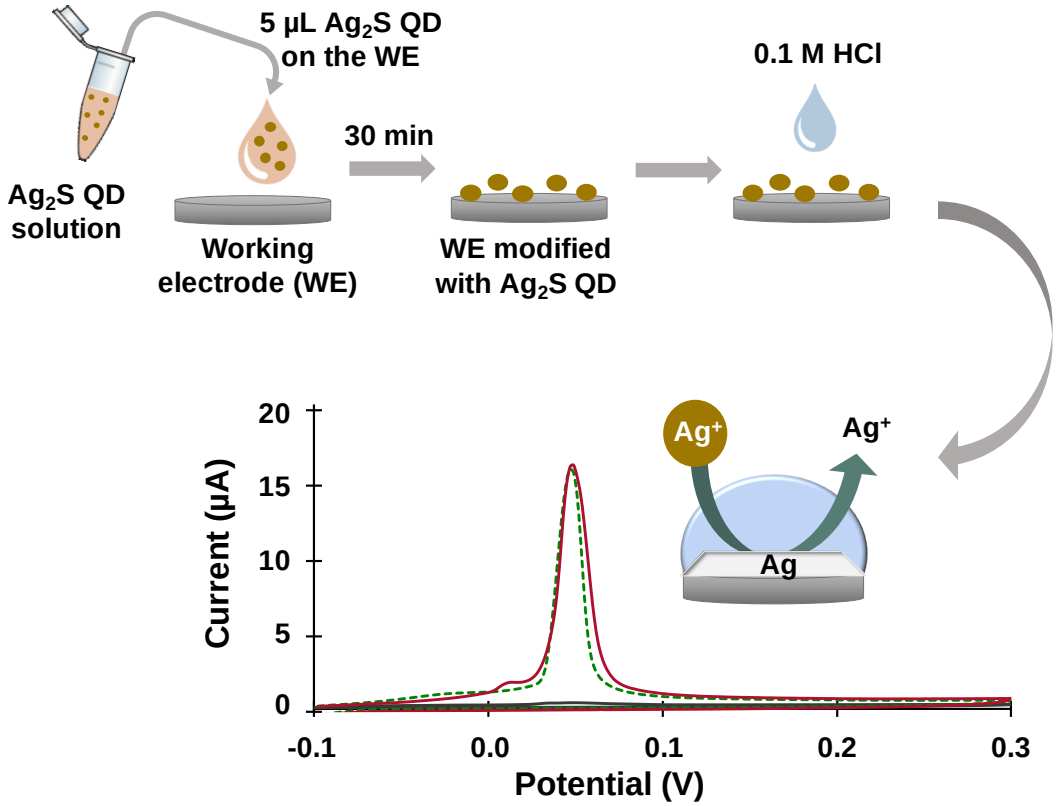

Fig. 2 Scheme of the experimental procedure for the Ag_2S QD quantification based on anodic stripping voltammetry. Cyclic voltammograms recorded from -0.1 V to +0.3 V at a scan rate of 50 $mV \cdot s^{-1}$ for the bare electrode (grey continuous line) and the electrode modified with suspensions of 1.40×10^{12} $QD \cdot mL^{-1}$ of 3-MPA-Ag_2S QD (continuous red line) and BA-Ag_2S QD (discontinuous green line) are shown

Typical voltammetric signals obtained for 1.40×10^{12} $QD \cdot mL^{-1}$ suspension of the synthesized Ag_2S QD (3-MPA-Ag_2S QD and BA-Ag_2S QD) are shown at **Fig. 2**. As can be observed, the peak current profiles are quite similar for both types of Ag_2S QD, being the peak current intensity slightly higher for the 3-MPA-Ag_2S QD.

3.2.2. Optimization of the method

The following parameters were optimized: (a) working potential; (b) electrodeposition time. Respective text and figures on optimizations are given at the ESM. In short, the following experimental conditions were found to give best results: (a) Best working potential: -0.3 V; (b) optimal Electrodeposition time: 60 s. As stated at the experimental section, the constant background of 0.8 μA coming from the silver present in the printed reference electrode is subtracted from all the analytical signals in the further quantification studies (both of Ag_2S QD and bacteria) under the optimized experimental conditions.

3.2.3. Quantification of Ag_2S QD with different surface coatings

The effect of the Ag_2S QD concentration on the analytical signal was evaluated for the two different surface coatings, following the optimized method. As shown in **Fig. 3**, the analytical signal increases when increasing the Ag_2S QD concentration adjusted to a linear relationship within a wide range (from 2.20×10^9 to 2.20×10^{12} QD·mL^{-1} for 3-MPA-Ag_2S QD and from 1.80×10^9 to 1.80×10^{12} QD·mL^{-1} for BA-Ag_2S QD), with good correlation coefficients, higher than 0.9975 in both cases. All the concentrations were adjusted into a linear relationship according to the following equations:

Peak current (μA) = 12.8×10^{-12} [3-MPA-Ag_2S QD] (QD·mL^{-1}) + 0.6 r = 0.9991

Peak current (μA) = 11.4×10^{-12} [BA-Ag_2S QD] (QD·mL^{-1}) + 0.2 r = 0.9975

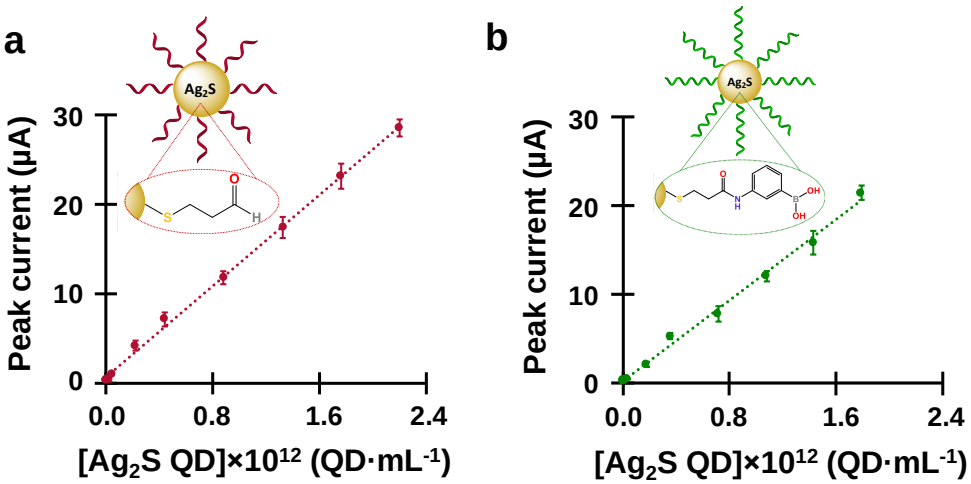

Fig. 3 Effect of the Ag_2S QD concentration on the analytical signal (voltammetric peak recorded at +0.06 V) for the different surface coatings evaluated: **(a)** 3-MPA-Ag_2S QD and **(b)** BA-Ag_2S QD, following the optimized method. Data are given as average ± SD (n=3)

The limit of detection (LOD), calculated as three times the standard deviation of the intercept divided by the slope, is 4.10×10^{10} QD·mL^{-1} for the 3-MPA-Ag_2S QD and 5.70×10^{10} QD·mL^{-1} for BA-Ag_2S QD. Additionally, the method shows a good reproducibility (RSD) of around 5% (n =3) (evaluated for 1.80×10^{12} QD·mL^{-1}).

The similar responses found for both QD in terms of sensitivity, reproducibility and limit of detection suggest that the different coatings are not affecting the electroactivity of the Ag_2S QD, which is of key relevance for their application as tags. The little decrease in the voltammetric signals noticed for the BA-Ag_2S QD is probably due to the bigger size of the coating agent which may shortly hinder the close contact of the silver with the electrode.

3.3. Bacteria quantification using Ag_2S QD: evaluation of the effect of different QD surface coating ligands

Well-stablished methods for specific determination of bacteria are commonly based on time consuming cells culturing or molecular biology techniques, giving qualitative or semi-quantitative information. Alternative techniques based on targeting intracellular proteins and nucleic acids also suffer of complex and long extraction procedures between other drawbacks. [21] In contrast, cell determination strategies based on the recognition of phospholipids and lipopolysaccharides expressed on bacterial cell walls allow to overcome such limitations. [22–24] In this context, nonspecific but selective bacteria assays based on the affinity of silver nanoparticles for such cell surface macromolecules (which is the basis of the anti-bacteria effect of silver) have been reported for quantitative analysis taking advantage of the electroactivity of silver. [25]

In our case, we have studied the ability of the novel Ag_2S QD to be used as tags for bacteria determination based on the silver-bacteria affinity and, even more interestingly, we have evaluated the effect of different QD surface coatings in the assay performance. *E. coli* bacteria was chosen as model for the demonstration of the proof-of-concept.

As detailed in the experimental section, different amounts of *E. coli* bacteria in the range from 10^{-1} and 10^{7} bacteria·mL^{-1} were incubated with a fix quantity of both QD, followed by centrifugation/purification before the electrochemical quantification of the silver linked to bacteria. The voltammetric peak current was then correlated with the concentration of *E. coli*.

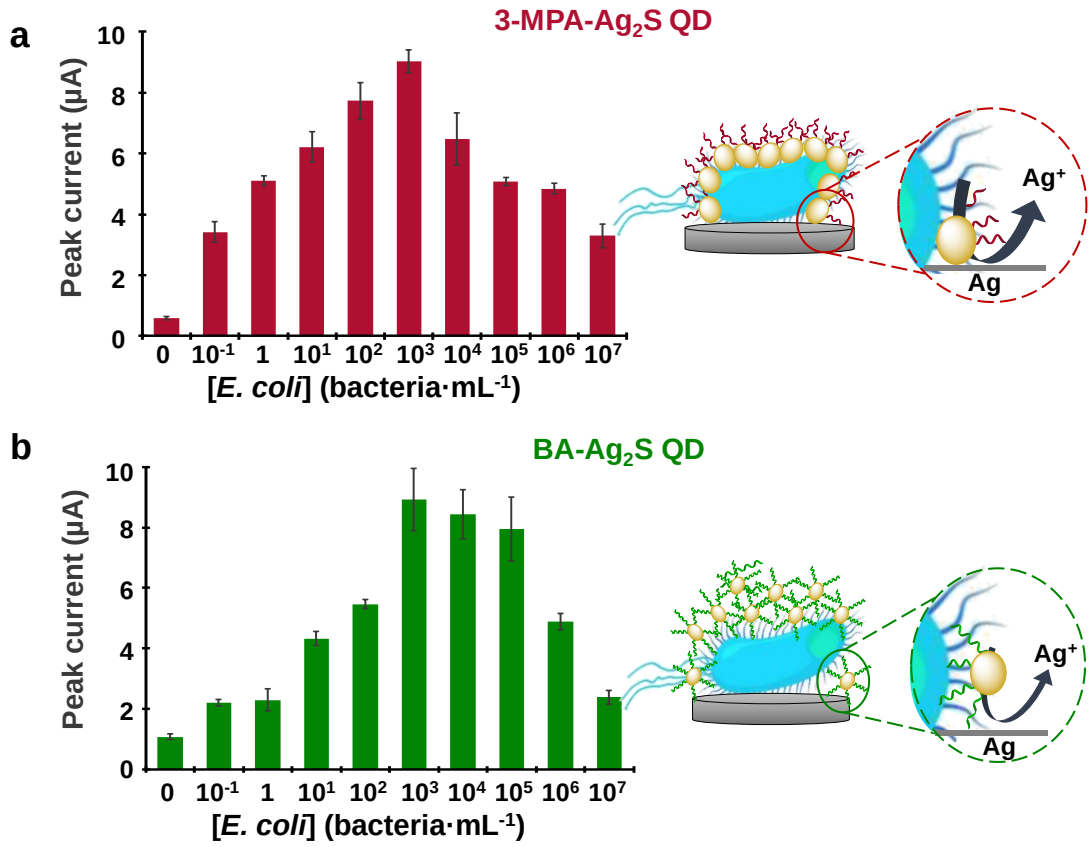

Fig. 4 Illustration of the *E. coli* determination strategy based on the incubation with **(a)** 3-MPA-Ag_2S QD and **(b)** BA-Ag_2S QD, and further electrochemical quantification of silver. Bar diagrams correspond to the voltammetric peak currents obtained for bacteria cells concentrations ranging from 10^{-1} to 10^{7} bacteria·mL^{-1}. Data are given as average ± SD (n=3)

As shown in **Fig. 4a** (left), in the case of the 3-MPA-Ag_2S QD, the peak current increases with the *E. coli* concentration up to 10^{3} bacteria·mL^{-1}. Such bacteria tagging can be attributed to the well-known affinity of silver nanoparticles for the phospholipids and lipopolysaccharides present of the bacterial cell walls, as expected. The short length of the 3-MPA ligand facilitates not only the contact of the silver with the cell walls but also the electronic transference during the silver quantification process, as depicted in the cartoon of **Fig. 4a** (right). The important decrease in the signal noticed for higher concentrations is probably due to the

saturation of the electrode with bacteria which blocks the electronic transference, what is in agreement with previous reports. [20, 25, 26] Quantitative evaluation of the presented data gave a logarithmic relationship between the analytical signal and the bacteria concentration in the range from 10^{-1} to 10^{3} bacteria·mL^{-1} adjusted to the following equation:

Peak current (μA) = 0.61 ln [*E. coli*] (bacteria·mL^{-1}) + 4.9 r = 0.998

The limit of detection, estimated as detailed above, was of 1 bacteria·mL^{-1} while the reproducibility of the method exhibited an RSD of 3% (n=3) for 1 bacteria·mL^{-1}.

In parallel, the response of the bacteria incubated with BA-Ag_2S QD was also evaluated. As shown in **Fig. 4b** (left), the profile of the electrochemical response is significantly different from the obtained for the 3-MPA covering, being needed higher amounts of bacteria for getting the same peak current values. The quantitative analysis also gives a shorter dynamic range of response (1-103 bacteria·mL^{-1}), adjusted to a logarithmic relationship with a quite poor correlation coefficient:

Peak current (μA) = 0.91 ln [*E. coli*] (bacteria·mL^{-1}) + 2.1 r = 0.977

This behaviour is probably in close relation with the characteristics of the BA ligand. On the one hand, the big-sized chains of this ligand may hinder the direct contact/interaction of the silver in the QD with the bacteria cell walls. However, the chemistry of the boronic acid in the ligand may be the responsible of the QD-bacteria linking in this case. It is known that the boronic acid interacts with different saccharides to form boronate esters. [27] Boronic acid has also shown reactivity with 1,2-diols or 1,3-diols in aqueous media to create five- or six-

membered cyclic esters, [28] and it has been widely used in the detection of mono- and polysaccharides, which are present in the peptidoglycan layer on the surface of bacteria cells. [28, 29] This means that BA-QD may be linked to bacteria cells via such chemically specific binding, as illustrated in **Fig. 4b** (right). However, this positive effect for the determination system is probably countered by steric issues: the long chains of the BA ligand are hindering the close contact of the Ag_2S QD with the electrode surface, leading to a decrease in the voltammetric response. All this makes the bacteria determination ability of the BA-coated Ag_2S QD worse than the observed for the less protected 3-MPA coated ones.

In order to elucidate the effect of the covering agent length on the bacteria determination system, a big-sized ligand but with no chemical affinity for the bacteria cell wall components was evaluated as control. Glutathione-modified Ag_2S QD were synthesized and assayed for that purpose. The results shown at the ESM (see **Fig. A4b**) evidence that such QD, although showing electroactivity for silver determination, do not exhibit any affinity for the bacteria cells. This demonstrates that the big coating of the QD is blocking the contact/interaction of the silver with the bacteria cell surface, suggesting that the response found for the BA-QD is mostly due to the chemical affinity of the boronic acid for the molecules on the bacteria cell surface.

3.4. Selectivity and specificity of the bacteria quantification assay

In or to test the selectivity of this determination strategy, a second model bacterial strain was evaluated following the same method. The current *versus*

concentration profile obtained by incubating *Salmonella* cells with 3-MPA-Ag_2S QD (see **Fig. 5a**, discontinuous bars) results in substantial similarity to the one observed with *E. coli* (see **Fig. 5a**, continuous bars) although reaching the maximum current intensity for lower *Salmonella* concentrations. Such different profile of response can be attributed to the analogous but dissimilar variety and type of surface functional macromolecules expressed on the cell walls. [30] Consequently, the average ratio between the number of electrochemical reporters per bacterial cell vary between both species. This behaviour, previously reported for PVP-coated AgNPs [25] demonstrates semispecific character of the assay, which has the potential ability to discriminate between different pathogenic organisms without the need of highly specific receptors like antibodies.

On the other hand, to evaluate the specificity of the bacteria determination method in complex samples, an assay on a *E. coli* suspension of 10^2 bacteria·mL^{-1} incubated with 3-MPA-Ag_2S QD in the presence of two different kind of potential interfering species was performed. Human serum was selected as representative matrix for biological/clinical applications while humic acid, the major component of river waters' total organic carbon, was chosen as representative matrix for environmental applications. As shown in **Fig. 5b**, a slight decrease in the analytical signal is observed for the assay performed in humic acid, suggesting the low interfering effect of such important environmental component. In contrast, the matrix of the human serum substantially affects the performance of the system, as evidenced by the approximately 50% decrease in the signal. This behaviour is probably due to the high abundance of proteins in the complex serum matrix which may unspecifically interact with the 3-MPA-Ag_2S QD.

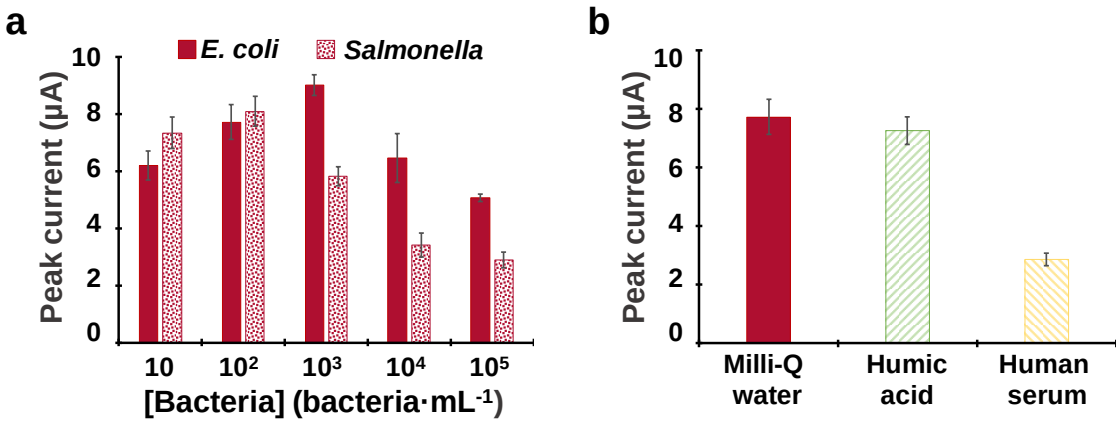

Fig. 5 **(a)** Voltammetric peak current profiles for bacteria, *E. coli* (continuous bars) and *Salmonella* (discontinuous bars) incubated with 3-MPA-Ag_2S QD; cell concentrations ranging from 10 to 10^5 bacteria·mL^{-1} and **(b)** Voltammetric peak currents recorded for assays performed on samples containing *E. coli* suspension of 10^2 bacteria·mL^{-1} in presence of two interfering species: humic acid (4 mg·L^{-1}) and human serum. Data are given as average ± SD (n=3)

The absence of Ag_2S QD aggregation in presence of multivalent cations was demonstrated in a previous work [16], where we studied the effect on the luminescence emission of AgS_2 of the presence of anions such as F^-, Cl^-, Br^-, I^-, NO_3^-, NO_2^-, SO_4^{2-}, SO_3^{2-}, $S_2O_3^{2-}$, SCN^-, PO_4^{3-}, S^{2-}, and cations including K^+, Zn^{2+}, Mg^{2+}, Cu^{2+}, Na^+, Fe^{2+}, Ca^{2+}, Mn^{2+}, Hg^{2+}, Cr^{6+}, As^{3+}. Results obtained showed that the presence of most of the relevant ions evaluated did not produce any significant effect on the emission of the synthesized Ag_2S QD, even when they are present at 1000 µM (the maximum concentration assayed). Such experiment is an evidence indicating that no aggregation of QD occur in the presence of such studied ions.

Overall, this method is a promising proof-of-concept alternative to traditional laboratory-based tests, with good sensitivity and short time and low cost of analysis. Apart from that, it can detect very low concentrations of bacteria just because of the high affinity between the Ag_2S QD and the cell walls, without the

need of any receptor, such as enzymes, antibodies or aptamers, simplifying enormously the method. In **Table 1** a comparison between different methods for bacteria determination based on different receptors and recognition systems is summarized, evidencing the good performance of our system, which also benefits of the above-mentioned advantages.

Table 1. An overview on recently reported methods for the determination of bacteria.

Reporter	Method	Figures of merit			Reference
		Analyte	Receptor	LOD	
Ag_2S QD	Cyclic voltammetry	*E. coli*	No receptor	0.4 bacteria·mL^{-1}	This work
AuAg nanoshells	Differential pulse voltammetry	*E. coli* and *Salmonella typhimurium (S. typ)*	No receptor	10^2 CFU·mL^{-1}	[25]
β-galactosidase-cationic AuNPs conjugate system	Colorimetry	*E. coli*	β-galactosidase	10^2 bacteria·mL^{-1}	[31]
β-galactosidase-cationic AuNPs conjugate system	Differential pulse voltammetry	*E. coli* and *Staphylococcus aureus (S. aureus)*	β-galactosidase	10^2 CFU·mL^{-1}	[32]
Bacterial Inhibition of Glucose Oxidase-catalyzed reaction	Colorimetric assay	*E. coli* and *S. aureus*	Glucose oxidase	7.48×10^3 CFU·mL^{-1} for *E. coli* and 3.3×10^3 CFU·mL^{-1} for *S. aureus*	[33]
Antibody-conjugated gold nanorod-based two-photon scattering	Two-Photon Rayleigh Scattering Spectroscopy	*E. coli* O157:H7	Anti-*E. coli* antibody-conjugated nanorods	50 CFU·mL^{-1}	[34]
Amino-terminated gold nanorods functionalised with antibodies	UV/Vis absorbance	*E. coli* O157: H7 and *S. typ*	Anti-*E. coli* and anti- *S. typ*	10^2 CFU·mL^{-1}	[35]
Antibody-conjugated oval shaped gold nanoparticles	Near infrared detection	*Salmonella*	Anti-Salmonella	$5.2\text{x}10^4$ bacteria	[36]
Antibody conjugated on a hyaluronic acid layer	Electrochemical impedance spectroscopy	*E. coli* O157:H7	anti-*E. coli* O157:H7 antibody	7 CFU·mL^{-1}	[37]
Antibody labelled with gold nanoparticles and magnetic beads	Chronoampero metry	*E. coli* O157:H7 in minced beef	*E. coli* O157 primary antibody	457 CFU·mL^{-1} in minced beef and 309	[26]

		and tap water		$CFU \cdot mL^{-1}$ in tap water	
ε-polylysine functionalized magnetic nanoparticles	Fluorescence	*E. coli* DH5α	Anti-*E. coli* DH5α antibody	98 $CFU \cdot mL^{-1}$	[24]
PDMS/paper/glass hybrid microfluidic biochip integrated with aptamer-functionalized graphene oxide	Fluorescence	*Lactobacillus acidophilus (L. acidophilus)*, *S. aureus* and *Salmonella enterica (S. enterica)*	Aptamers for each bacteria	11 $CFU \cdot mL^{-1}$ for L. acidophilus, 800 $CFU \cdot mL^{-1}$ for S. aureus and 61 $CFU \cdot mL^{-1}$ for S. enterica	[38]
Fluorophore 5-carboxyfluorescein labelled aptamer on graphene oxide	Fluorescence	*S. typ.*	Aptamer for *S. typ*	100 $CFU \cdot mL^{-1}$	[39]

4. CONCLUSION

In this work, we report for the first time the electrochemical quantification of novel NIR-emitting Ag_2S QD as well as their application as novel electrochemical reporters for the rapid determination of bacterial cells on screen-printed carbon electrodes. Interestingly, studies carried out with different Ag_2S QD surface ligands/stabilizers show that short length ligands with no affinity for the bacteria cells exhibit better performance than long length ones. Such findings suggest that the less-protected silver surface is available to interact with the cell surface walls, being such interaction blocked for the more protected QD. Long length ligands with chemical affinity for the macromolecules expressed on the bacteria cell walls also show worse performance, suggesting that steric effects affecting the voltammetric detection play a key role in the determination system. Overall, this method based on novel Ag_2S QD represents a promising proof-of-concept for rapid and sensitive bacteria quantification able to compete with traditional costly and time-consuming laboratory analyses. The non-specific interaction between

Ag_2S QD and the bacterial cells avoids the need any receptor such as enzymes, antibodies or aptamers, which results in a more rapid and cost-effective system.

ACKNOWLEDGEMENTS

This work has been supported by the FC-GRUPIN-ID/2018/000166 and FC-GRUPIN-ID/2015/021 projects from the Asturias Regional Government and the CTQ2017–86994-R, CTQ2016–79412-P and CTQ2014–58826-R projects from the MINECO (Spain). O. Amor-Gutiérrez thanks the University of Oviedo for the award of a grant “Ayudas para la realización de tesis doctorales” (PAPI-18-PF-13). A. Iglesias-Mayor thanks the MECD (Spain) for the award of a FPU Grant (FPU2014/04686). A. de la Escosura-Muñiz acknowledges the MICINN (Spain) for the “Ramón y Cajal” Research Fellow (RyC-2016-20299). F. Parra laboratory was funded by the Municipality of Ribera de Arriba/La Ribera (Asturias, Spain). Authors would like to acknowledge the technical support provided by Servicios Científico-Técnicos de la Universidad de Oviedo (Alaa Adawy at the laboratory of HR-TEM).

REFERENCES

1. Editorial (2014) Nanocrystals in their prime. Nat Nanotechnol 9:325. https://doi.org/10.1038/nnano.2014.101

2. Ekimov AI, Onushchenko AA (1982) Quantum size effect in 3D microscopic semiconductor crystals. JETP Lett 34:345–348

3. Alivisatos AP (1996) Semiconductor clusters, nanocrystals, and Quantum

Dots. Science (80-) 271:933–937

4. Murray CB, Norris DJ, Bawendi MG (1993) Synthesis and Characterization of Nearly Monodisperse CdE (E = S, Se, Te) Semiconductor Nanocrystallites. J Am Chem Soc 115:8706–8715. https://doi.org/10.1021/ja00072a025

5. Grabolle M, Ziegler J, Merkulov A, et al (2008) Stability and fluorescence quantum yield of CdSe-ZnS quantum dots - Influence of the thickness of the ZnS shell. Ann N Y Acad Sci 1130:235–241. https://doi.org/10.1196/annals.1430.021

6. Montoro Bustos AR, Trapiella-Alfonso L, Encinar JR, et al (2012) Elemental and molecular detection for Quantum Dots-based immunoassays: A critical appraisal. Biosens Bioelectron 33:165–171. https://doi.org/10.1016/j.bios.2011.12.046

7. Trapiella-Alfonso L, Montoro Bustos AR, Ruiz Encinar J, et al (2011) New integrated elemental and molecular strategies as a diagnostic tool for the quality of water soluble quantum dots and their bioconjugates. Nanoscale 3:954–957. https://doi.org/10.1039/c0nr00822b

8. Montoro Bustos AR, Encinar JR, Fernández-Argüelles MT, et al (2009) Elemental mass spectrometry: A powerful tool for an accurate characterisation at elemental level of quantum dots. Chem Commun 3107–3109. https://doi.org/10.1039/b901493d

9. Amelia M, Impellizzeri S, Monaco S, et al (2011) Structural and size effects on the spectroscopic and redox properties of cdse nanocrystals in solution: The role of defect states. ChemPhysChem 12:2280–2288.

https://doi.org/10.1002/cphc.201100300

10. Haram SK, Quinn BM, Bard AJ (2001) Electrochemistry of CdS nanoparticles: A correlation between optical and electrochemical band gaps [5]. J Am Chem Soc 123:8860–8861. https://doi.org/10.1021/ja0158206

11. Bard AJ, Ding Z, Myung N (2005) Electrochemistry and electrogenerated chemiluminescence of semiconductor nanocrystals in solutions and in films. Struct Bond 118:1–57. https://doi.org/10.1007/b137239

12. Wang J, Liu G, Polsky R, Merkoçi A (2002) Electrochemical stripping detection of DNA hybridization based on cadmium sulfide nanoparticle tags. Electrochem commun 4:722–726. https://doi.org/10.1016/S1388-2481(02)00434-4

13. de la Escosura-Muñiz A, Ambrosi A, Merkoçi A (2008) Electrochemical analysis with nanoparticle-based biosystems. TrAC - Trends Anal Chem 27:568–584. https://doi.org/10.1016/j.trac.2008.05.008

14. Zhao P, Xu Q, Tao J, et al (2018) Near infrared quantum dots in biomedical applications: current status and future perspective. Wiley Interdiscip Rev Nanomedicine Nanobiotechnology 10:1–16. https://doi.org/10.1002/wnan.1483

15. Gu YP, Cui R, Zhang ZL, et al (2012) Ultrasmall near-infrared Ag 2Se quantum dots with tunable fluorescence for in vivo imaging. J Am Chem Soc 134:79–82. https://doi.org/10.1021/ja2089553

16. Llano-Suárez P, Bouzas-Ramos D, Costa-Fernández JM, et al (2019)

Near-infrared fluorescent nanoprobes for highly sensitive cyanide quantification in natural waters. Talanta 192:463–470. https://doi.org/10.1016/j.talanta.2018.09.073

17. Drain PK, Hyle EP, Noubary F, et al (2014) Diagnostic point-of-care tests in resource-limited settings. Lancet Infect Dis 14:239–249. https://doi.org/10.1016/S1473-3099(13)70250-0

18. WHO (2017) Global action plan on antimicrobial resistance. Who 1–28

19. Hermanson GT (2013) Bioconjugate techniques, Third Edit. Elsevier Inc., Jamestown Road, London

20. Espinoza-Castañeda M, de la Escosura-Muñiz A, González-Ortiz G, et al (2013) Casein modified gold nanoparticles for future theranostic applications. Biosens Bioelectron 40:271–276. https://doi.org/10.1016/j.bios.2012.07.042

21. Tamerat N, Muktar Y (2016) Application of Molecular Diagnostic Techniques for the Detection of E. coli O157:H7: A Review. J Vet Sci Technol 7:. https://doi.org/10.4172/2157-7579.1000362

22. Sepunaru L, Tschulik K, Batchelor-McAuley C, et al (2015) Electrochemical detection of single E. coli bacteria labeled with silver nanoparticles. Biomater Sci 3:816–820. https://doi.org/10.1039/c5bm00114e

23. Feng ZV, Gunsolus IL, Qiu TA, et al (2015) Impacts of gold nanoparticle charge and ligand type on surface binding and toxicity to Gram-negative and Gram-positive bacteria. Chem Sci 6:5186–5196.

https://doi.org/10.1039/c5sc00792e

24. Wu X, Lai T, Jiang J, et al (2019) An on-site bacterial detection strategy based on broad-spectrum antibacterial ε-polylysine functionalized magnetic nanoparticles combined with a portable fluorometer. Microchim Acta 186:526. https://doi.org/10.1007/s00604-019-3632-1

25. Russo L, Leva Bueno J, Bergua JF, et al (2018) Low-cost strategy for the development of a rapid electrochemical assay for bacteria detection based on AuAg nanoshells. ACS Omega 3:18849–18856. https://doi.org/10.1021/acsomega.8b02458

26. Hassan A-RHA-A, de la Escosura-Muñiz A, Merkoçi A (2015) Highly sensitive and rapid determination of Escherichia coli O157:H7 in minced beef and water using electrocatalytic gold nanoparticle tags. Biosens Bioelectron 67:511–515. https://doi.org/10.1016/j.bios.2014.09.019

27. Resendez A, Halim MA, Singh J, et al (2017) Boronic acid recognition of non-interacting carbohydrates for biomedical applications: Increasing fluorescence signals of minimally interacting aldoses and sucralose. Org Biomol Chem 15:9727–9733. https://doi.org/10.1039/c7ob01893b

28. Li J, Wu H, Santana I, et al (2018) Standoff Optical Glucose Sensing in Photosynthetic Organisms by a Quantum Dot Fluorescent Probe. ACS Appl Mater Interfaces 10:28279–28289. https://doi.org/10.1021/acsami.8b07179

29. Whyte GF, Vilar R, Woscholski R (2013) Molecular recognition with boronic acids-applications in chemical biology. J Chem Biol 6:161–174. https://doi.org/10.1007/s12154-013-0099-0

30. Chen J, Andler SM, Goddard JM, et al (2017) Integrating recognition elements with nanomaterials for bacteria sensing. Chem Soc Rev 46:1272–1283. https://doi.org/10.1039/c6cs00313c

31. Miranda OR, Li X, Garcia-Gonzalez L, et al (2011) Colorimetric bacteria sensing using a supramolecular enzyme-nanoparticle biosensor. J Am Chem Soc 133:9650–9653. https://doi.org/10.1021/ja2021729

32. Chen J, Jiang Z, Ackerman JD, et al (2015) Electrochemical nanoparticle-enzyme sensors for screening bacterial contamination in drinking water. Analyst 140:4991–4996. https://doi.org/10.1039/c5an00637f

33. Sun J, Huang J, Li Y, et al (2019) A simple and rapid colorimetric bacteria detection method based on bacterial inhibition of glucose oxidase-catalyzed reaction. Talanta 197:304–309. https://doi.org/10.1016/j.talanta.2019.01.039

34. Singh AK, Senapati D, Wang S, et al (2009) Gold Nanorod Based Selective Identification ofEscherichia coli Bacteria Using Two-Photon Rayleigh Scattering Spectroscopy. ACS Nano 3:1906–1912

35. Wang C, Irudayaraj J (2008) Gold nanorod probes for the detection of multiple pathogens. Small 4:2204–2208. https://doi.org/10.1002/smll.200800309

36. Wang S, Singh AK, Senapati D, et al (2010) Rapid colorimetric identification and targeted photothermal lysis of Salmonella bacteria by using bioconjugated oval-shaped gold nanoparticles. Chem - A Eur J 16:5600–5606. https://doi.org/10.1002/chem.201000176

37. Joung CK, Kim HN, Im HC, et al (2012) Ultra-sensitive detection of pathogenic microorganism using surface-engineered impedimetric immunosensor. Sensors Actuators, B Chem 161:824–831. https://doi.org/10.1016/j.snb.2011.11.041

38. Zuo P, Li X, Dominguez DC, Ye BC (2013) A PDMS/paper/glass hybrid microfluidic biochip integrated with aptamer-functionalized graphene oxide nano-biosensors for one-step multiplexed pathogen detection. Lab Chip 13:3921–3928. https://doi.org/10.1039/c3lc50654a

39. Duan YF, Ning Y, Song Y, Deng L (2014) Fluorescent aptasensor for the determination of Salmonella typhimurium based on a graphene oxide platform. Microchim Acta 181:647–653. https://doi.org/10.1007/s00604-014-1170-4